

Dalton Transactions

Accepted Manuscript



This is an *Accepted Manuscript*, which has been through the Royal Society of Chemistry peer review process and has been accepted for publication.

Accepted Manuscripts are published online shortly after acceptance, before technical editing, formatting and proof reading. Using this free service, authors can make their results available to the community, in citable form, before we publish the edited article. We will replace this *Accepted Manuscript* with the edited and formatted *Advance Article* as soon as it is available.

You can find more information about *Accepted Manuscripts* in the [Information for Authors](#).

Please note that technical editing may introduce minor changes to the text and/or graphics, which may alter content. The journal's standard [Terms & Conditions](#) and the [Ethical guidelines](#) still apply. In no event shall the Royal Society of Chemistry be held responsible for any errors or omissions in this *Accepted Manuscript* or any consequences arising from the use of any information it contains.



CuAAC Click Reactions for the Design of Multifunctional Luminescent Ruthenium Complexes

N. Zabarska,^a A. Stumper^a and S. Rau^{a*}

Received 00th January 20xx,
Accepted 00th January 20xx

DOI: 10.1039/x0xx00000x

www.rsc.org/

CuAAC (Cu(I) catalyzed azide-alkyne cycloaddition) click chemistry emerged as a versatile tool in the development of photoactive ruthenium complexes with multilateral potential applicability. In this contribution we discuss possible synthetic approaches towards CuAAC reactions with ruthenium(II) polypyridine complexes and their differences with respect to possible applications. We focus on two main application possibilities of the click-coupled ruthenium assemblies. New results within the development of ruthenium based photosensitizers for the field of renewable energy supply, i.e. DSSC's (dye-sensitized solar cells) and artificial photocatalysis for the production of hydrogen, or for anticancer photodynamic therapeutic applications are reviewed.

Introduction

In the last decades a special interest emerged for the development of photoactive hybrids that can be applied in dye sensitized solar cells (DSSC's), catalysis and designing molecules for biological applications. At that, ruthenium complexes with chelating ligands are very attractive photoactive hybrids, due to their opulent and diversely tunable photochemistry.¹ Within the context of building multifunctional metal complexes, the concept of "click chemistry" is of great interest. It has been established by K.B. Sharpless in 2001.² Out of versatile examples for click reactions, our work focuses on particularly the copper(I) catalyzed azide-alkyne cycloaddition (CuAAC).³ At this reaction, substances with different properties **A** (functionalized with an alkyne-group) and **B** (functionalized with an azide-group) are combined for the formation of **C** with 1,2,3-triazole as the connecting link (see Figure 1). Remarkably, only the 1,4-substituted triazole is formed. If working under copper-free conditions (azide-alkyne Huisgen cycloaddition), both the 1,4- and the 1,5-substitution would occur. Noteworthy, ruthenium(II) polypyridine complexes $[\text{Ru}(\text{bpy})_3]^{2+}$ are perfectly suitable for CuAAC click reactions, since pyridines were shown to enhance the CuAAC reaction kinetics.⁴ However, it should be taken into account, that changing the ligand sphere of $[\text{Ru}(\text{bpy})_3]^{2+}$ complexes within the context of CuAAC click reactions might change the photophysical properties.

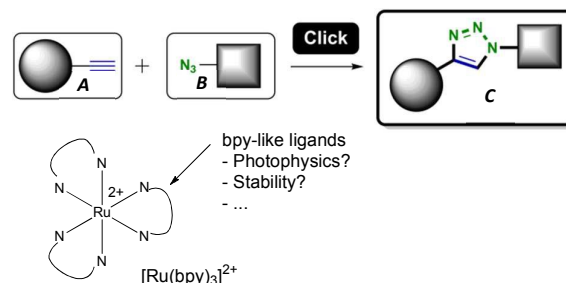


Fig. 1 At the top: general scheme of the CuAAC click reaction. A functionalized alkyne (**A**) reacts with a functionalized azide (**B**) forming a 1,4-substituted triazole (**C**). At the bottom: structure of $[\text{Ru}(\text{bpy})_3]^{2+}$ complexes with bpy as a derivative of 2,2'-bipyridine.

1. Photophysical activity of ruthenium complexes

Ruthenium complexes, in particular $[\text{Ru}(\text{bpy})_3]^{2+}$ complexes, have outstanding photophysical properties, such as absorption of visible light, relatively intensive and long-lived luminescence, long lifetime of the excited state and distinguished excited-state reactivity.^{5, 6} Their photoactivity is depicted in the Jablonski diagram (see Figure 2).

^a Institute of Inorganic Chemistry I, Ulm University, Albert-Einstein-Allee 11, 89081 Ulm, Germany. E-mail: Sven.Rau@uni-ulm.de.

† Footnotes relating to the title and/or authors should appear here.

Electronic Supplementary Information (ESI) available: [details of any supplementary information available should be included here]. See DOI: 10.1039/x0xx00000x

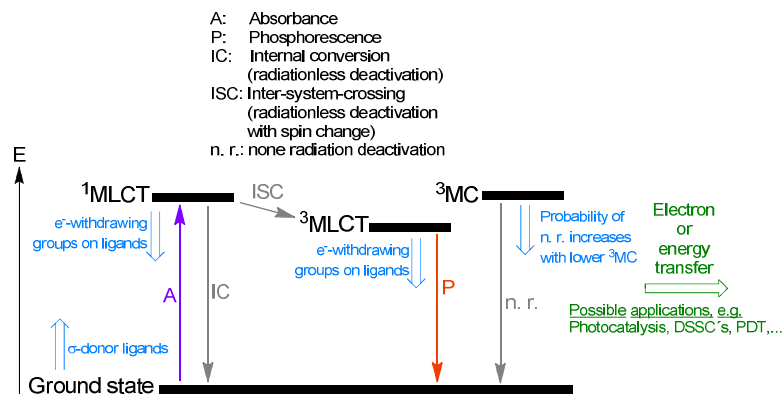


Fig. 2 Jablonski diagram for

the photophysical properties of ruthenium complexes.

Most important feature is the absorbance (A) of visible light, leading to an electronic metal-to-ligand-charge-transfer (MLCT) with typical ϵ values of $10000 \text{ M}^{-1}\text{cm}^{-1}$.¹ The MLCT excitation occurs at around 450 nm generating the $^1\text{MLCT}^*$ state. Thereafter, a fast conversion into the triplet state $^3\text{MLCT}^*$ occurs via fast inter-system-crossing (ISC), due to the heavy metal effect of ruthenium. Then, the $^3\text{MLCT}^*$ is usually deactivated by phosphorescence with a typical emission lifetime of $\tau \approx 0.7 \mu\text{s}$ and emission quantum yield Φ_{EM} of around 0.06 under deaerated conditions. Respectively, these values are lower in an oxygen saturated solvent with $\tau \approx 0.16 \mu\text{s}$ and $\Phi_{\text{EM}} \approx 0.02$.^{1, 7, 8} The lower phosphorescence intensity, due to presence of oxygen results from the conversion of oxygen in its ground state into the reactive singlet oxygen $^1\text{O}_2$ with typical singlet oxygen quantum yields Φ_{Δ} of around 90% in methanol and 40% in water respectively.⁹ Employment of good σ -donor ligands or electron-withdrawing groups, decrease the energy gap between the orbitals π_{M} and π_{L}^* . Thus, excitation of the ruthenium complexes would be possible with longer wavelengths, which is aspired, e.g. in therapeutic applications.

As long as $^3\text{MLCT}$ is the lowest energetic state, phosphorescence occurs. If ^3MC lies below $^3\text{MLCT}$, radiationless deactivation to the ground state or ligand dissociation takes place. Upon presence of acceptor molecules, electron or energy transfer can occur from the $^3\text{MLCT}$ or the ^3MC state, which is a key point for possible applications, such as photocatalysis, dye sensitized solar cells (DSSC's) and photodynamic therapy (PDT).

2. CuAAC Click reactions with Ru(II) polypyridine complexes

Regarding ruthenium complexes, the CuAAC click reaction can be carried out via the "click to chelate"¹⁰, "click then chelate"¹¹ or "chelate then click"¹¹ approach. At "click to chelate", first a click reaction is performed with a substance of desired property, forming a triazole containing chelating ligand. Then this ligand is chelated to a metal center with triazole as one of the chelating units (see Figure 3).^{10, 12-19} Upon "click then chelate" first a chelating ligand is clicked with a substance of desired property. Afterwards the ligand is chelated to the metal center. Here, the triazole unit does not take part at the chelation. (see Figure 3).^{11, 20}

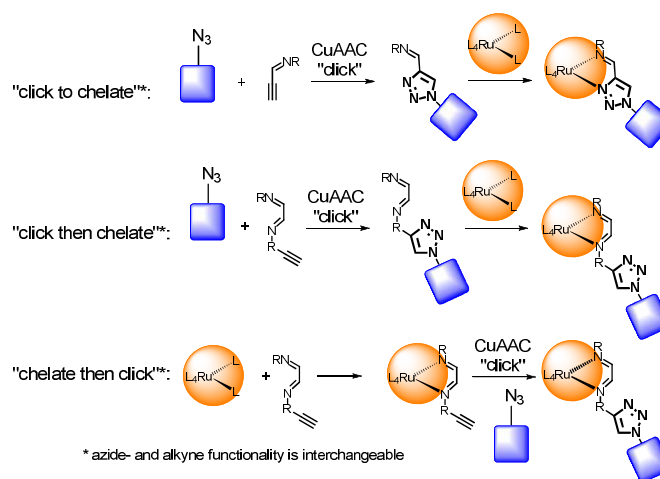


Fig. 3 CuAAC click reaction approaches with ruthenium complexes.

At the “chelate then click” approach, first a ligand with whether an azide - or alkyne functionality is chelated to the metal center. Thereafter the CuAAC click reaction is performed with the substance of desired property (see Figure 3).¹¹ All approaches yield the required multifunctional assembly.

3. Synthetic examples for CuAAC click reaction approaches with ruthenium complexes

Which CuAAC approach is chosen, depends on the substances that are applied. In case the transition metal is expensive, the “click to chelate” or “click then chelate” approach is preferable, since the metal complex is utilized only in the last step. However, if sensitive substances, e.g. biological groups, are being applied, it is advisable to attach them via the “chelate then click” approach, since they may not withstand the rather harsh conditions upon a typical chelation reaction.²¹ Hence sensitive groups are attached only during gentle CuAAC click conditions.

3.1. “Click to chelate”

Schubert et al. used the “click to chelate” approach for the formation of a ruthenium based metallopolymer **1** with large extinction coefficients and a high luminescence quantum yield of $\Phi_{EM} = 0.97$. (see Figure 4).¹³ First the ligand was synthesized via CuAAC and afterwards chelated to the ruthenium center. Nevertheless, it has to be considered that metal complexes generated within “click to chelate” may lose their luminescence, due to low σ -donor features of the triazole as a chelating ligand.²² This fact may be utilized to affect the luminescence intensity of the ruthenium complex by substitution of the chelating ligand, as depicted in Figure 5.²³ Here substitution of the pyridine unit at position 5 leads to enhanced or reduced emission intensity depending on whether an electron withdrawing or electron donating group is introduced respectively.

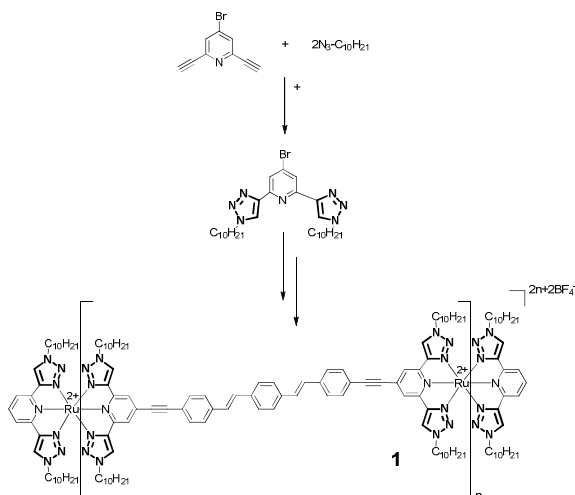


Fig. 4 Synthesis of complex **1**.

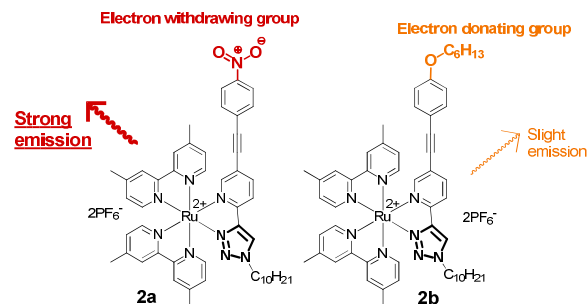


Fig. 5 Different emission intensities with respect to the electronic properties of the ligand.

3.2. “Click then chelate”

The “click then chelate” strategy was shown, for example, by Aukauloo et al.²⁰ A chelating bpy ligand was coupled to organic electron accepting or -donating groups via CuAAC (CuSO₄/sodium ascorbate) under standard conditions. Notably, coupling of NDI required heating at 130°C for 2 days. Afterwards, the ligand was coordinated to a ruthenium(II) polypyridine forming complexes **3a-c**. An efficient electron transfer through the triazole linker could be verified.

Regularly, investigations are carried out, using both the “click then chelate” and the “chelate then click” approach for the generation of the same target molecule. P. Elliott, for instance, developed the synthesis of triazole substituted Ru-bpy compounds (**4a-c**), as shown in Figure 7.²⁴ Herewith, a conjugation with luminescent pyrene or redox active ferrocene was possible. Both synthesis routes were performed within similar yields between 47-80%. Conditions of the click reactions are listed in Table 1.

Recently, an alkyne functionalized bipyridine could be connected with phosphonic acid anchoring groups via CuAAC (see Table 1). With these results essential distance control between the coordination sphere and semiconducting metal oxide surface is feasible by the insertion of a defined number of phenylene linkers (see **5a-b** in Figure 8). Hence, **5a-b** are suitable for the “click then chelate” approach.²⁵

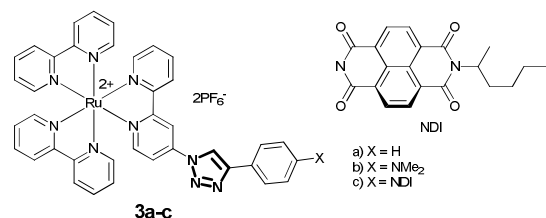


Fig. 6 Complexes **3**

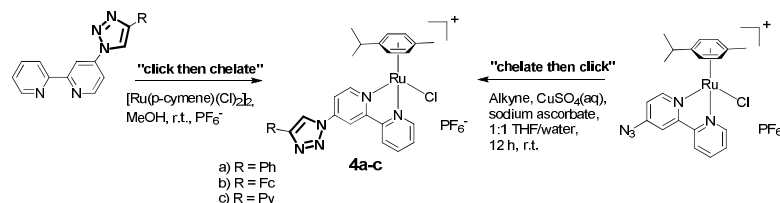


Fig. 7 Synthesis of **4a-c** via “click then chelate” or “chelate then click”.

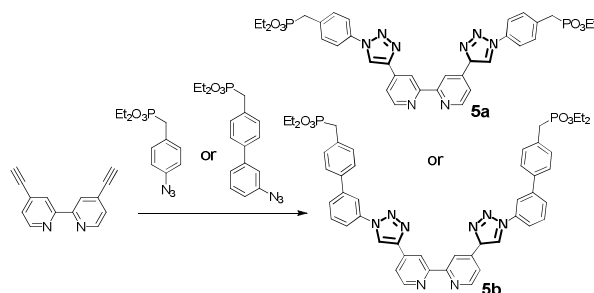


Fig. 8 Introduction of posphonic acid anchoring groups to a chelating bipyridine ligand via CuAAC with varying distances.

3.3. “Chelate than click”

At the „chelate then click” approach, first the ruthenium complex has to be functionalized whether with an azide or an alkyne group as shown above in Figure 7, where a sandwich type ruthenium complex was first substituted with an azide functionality leading to complex **4**. But, so far, in the case of octahedral $[\text{Ru}(\text{bpy})_3]^{2+}$ type complexes, there are only few examples in literature with efficient azide functionalization and subsequent succeeding performance of a click reaction. This might be explained by the instability of this functional group which can be sensitive to water, heat and shock, depending on the molecular linkage. One possibility for the stabilization of the azide group is the incorporation of an intermediary methylene spacer at the Ru(II) bipyridine core (see complex **6**). Thereafter, a successful CuAAC click reaction with standard conditions ($\text{CuSO}_4/\text{NaAsc}$) could be performed as well (see Table 1).²⁶

More examples are found for alkyne substituted complexes. Alkyne functionalized $[\text{Ru}(\text{bpy})_3]^{2+}$ complexes **7a-c** can be obtained via typical coordination reactions ($\text{EtOH}/\text{H}_2\text{O}$, Δ) between an alkyne functionalized bipyridine $\text{bpy}(\text{CCH})_m$ and the ruthenium precursor $\text{Ru}(\text{R-bpy})_2\text{Cl}_2$ with R = H or *tert*-butyl.²⁷

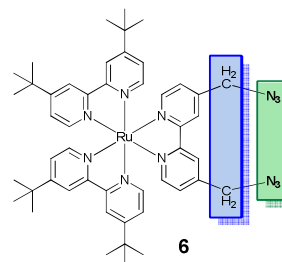


Fig. 9 Complex **6**

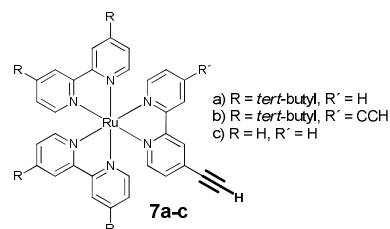


Fig. 10 Complexes **7a-c**

However, the above shown synthesis procedure of **7a-c** is accompanied by wasteful side reactions (see Figure 11).²⁷ Thereby, the Ru(II) center reacts with the alkyne group, resulting in a degradation of the alkyne group. This leads to a significant yield drop down to 20% of the actually desired alkyne functionalized ruthenium complexes **7a-c**.

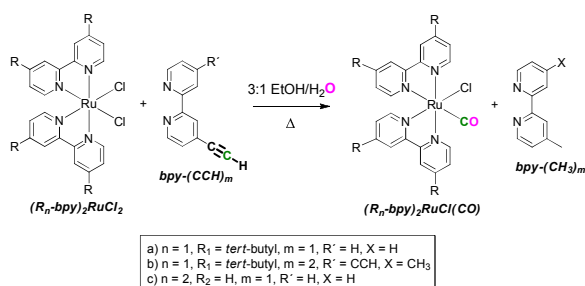


Fig. 11 Degradation of the alkyne group at the complexation reaction between an alkyne-bipyridine and $(R_n\text{-bpy})_2\text{RuCl}_2$. All charges and ions are omitted for clarity.

Sophisticated synthesis methods have been applied in order to avoid the above mentioned side reactions. Analogical ruthenium complexes were synthesized by Aukauloo, using Ag^+ ions for the promotion of the coordination reaction and simultaneous suppressing of the side reactions.²⁸ After formation of an alkyne functionalized $[\text{Ru}(\text{bpy})_3]^{2+}$ complex with a yield of 91%, no further purification steps were needed besides washing with water and diethylether. Afterwards, different azides were clicked via CuAAC (see Figure 12 and Table 1) forming **8a-c**. Interestingly, the only structural difference between complex **8** and **3** (shown in Figure 6) consists only in the connectivity through the N- or C-atom. However, the photophysical properties partly differ. Whereas both complexes absorb at $\lambda_{\text{MLCT}} \approx 460$ nm, their luminescence vary. The C-substituted complexes **8a-c** emit light at around 620 nm with varying luminescence quantum yields $\Phi_{\text{EM}} = 0.089$ (**8a**), 0.039 (**8b**) and 0.049 (**8c**). Upon substitution via the N1 atom (**3a-c**), the emission is bathochromically shifted around 10 nm. In the case of **3a** and **3c**, Φ_{EM} increases up to 0.097 and 0.140 respectively. In contrast, Φ_{EM} of **3b** drops down to 0.009, due to generation of a nonemissive charge-transfer state $^3\text{ILCT}$.^{20, 28}

Another interesting option was shown by Stahl et al with the usage of protecting groups (PG's).²⁹ An alkyne functionalized ruthenium(II) polypyridine complex **9** was synthesized within a stepwise build up starting from a bromo-substituted ruthenium complex. A triisopropylsilyl (TIPS) protected alkyne functionality was introduced via Sonogashira reaction. Surprisingly, TIPS could not be removed using typical deprotecting agents such as TBACl. Removal was only reached using AgF .

However, the above shown approaches employing Ag^+ ions cannot be applied for medical applications, since Ag^+ ions are known to be toxic.^{30, 31} Notably, Schanze et al. prepared a phenanthroline-alkyne (phen-alkyne) substituted $[\text{Ru}(\text{bpy})_3]^{2+}$ complex by analogous complexation reaction shown above in Figure 10 without using Ag^+ . In spite, that purification by column chromatography was needed after the synthesis, **10** was obtained within a yield of 90%, which is considerably higher compared to **7a-c**. Obviously, generation of side products is substantially lower, tentatively due to reduction of the reactivity between the Ru(II) center and the alkyne group

upon intermediary integration of a phenyl group between the alkyne and the chelating pyridine unit. Subsequently, a polymeric chromophore chain (**11a-b**) was generated by coupling with a polymeric azide chain via CuAAC (see Figure 14 and Table 1).³² **11a-b** serves as an efficient light harvesting array, with a molar extinction coefficient of $350000 \text{ M}^{-1}\text{cm}^{-1}$. Another good method for the introduction of an alkyne group without side products was shown with the synthesis of complex **12** with a yield of 85%. It was prepared by amidation of propargyl amine to a carboxyl functionalized Ru(II) complex (see Figure 15).³³

In the following, we discuss selected CuAAC click reactions that were used to build photoactive ruthenium complexes with interesting applications whether in the field of clean energy supply (i.e. DSSC's and catalysis) or photodynamic therapeutic applications.

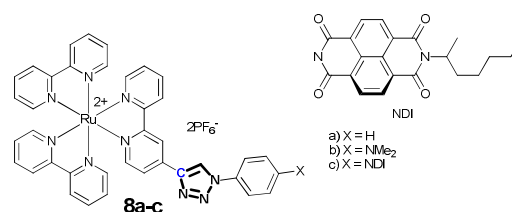


Fig. 12 Complexes **8a-c**.

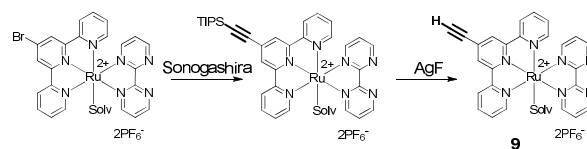


Fig. 13 Stepwise build-up of an alkyne functionalized ruthenium complex starting from a bromo-terpyridine substituted ruthenium(II) complex.

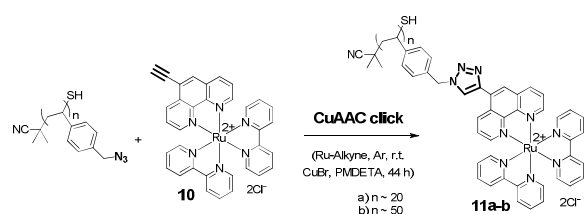


Fig. 14 CuAAC click between an azide functionalized polymeric chain and alkyne functionalized ruthenium(II) complexes.

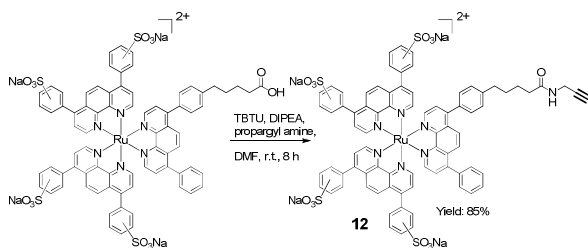


Fig. 15 Introduction of an alkyne functionality to a carboxyl-substituted ruthenium(II) polypyridine complex.

4. Photosensitizers generated by CuAAC for the development of energy conversion schemes

In order to ensure the world's increasing demand for energy, renewable resources like solar energy need to be harvested. Within this content, devices like solar cells are intensively investigated. There, efficient photon harvesting from sunlight is a sovereign aim. The concept of click chemistry can be used to build-up extensive molecular structures, which can collect photons and subsequently generate a photoinduced electron transfer. The so obtained electron transfer can be applied whether for the development of dye sensitized solar cells (DSSC's) or catalysis of energy storage products, such as hydrogen (obtained from water reduction and -oxidation). Additionally, photocatalysis can be employed by conversion of the greenhouse gas CO_2 to useful carbon sources, such as CO. The important electronic processes for ruthenium complexes are summarized in the Jablonski diagram (see Figure 2).³⁴

4.1. Applications for dye sensitized solar cells (DSSC's)

Dye sensitized solar cells (DSSC's), which are also called "Grätzel cells" absorb visible sunlight and convert it into electric energy. A schematic representation of the working principle is shown in Figure 16.³⁵ Initially, the dye molecule is electronically excited by visible light. Afterwards one excited electron is transferred from the dye to the conduction band of mesoporous semi conducting TiO_2 , which is adsorbed on the anode. Thus an external electron flux is generated towards the cathode, which is coated with platinum particles. From there the electron is handed to the electrolyte, which is usually an I_3^-/I^- system. Finally, the dye is recovered by the electrolyte closing the electron flux cycle. Since the first report about a high efficiency (7-8%) DSSC by Grätzel in 1991, the advancement of DSSC's is being extensively enabled by varying the dye, electrolyte or the mesoporous metal oxide films. Regarding the electrolyte system, a cobalt polypyridine derivative was recently found to be more efficient compared to the standard I_3^-/I^- .³⁶ The dye has to fulfill numerous functions, i.e. chemically strong linkage to the TiO_2 surface, high molar absorption coefficients, directional photoinduced electron transfer to TiO_2 , high stability in the one electron oxidized state and ease of reduction by the electrolyte

component. Hereafter, we show the development of ruthenium based dyes using CuAAC click reactions.

A number of CuAAC click reactions has been used to generate ruthenium based dyes for DSSC's applications. The "click then chelate" approach, for example, was used by Galoppini et al. for the generation of "star" shaped ruthenium complexes **13a-b** (see Figure 17).³⁷ They could be bound to semiconducting TiO_2 , which is an important issue regarding DSSC's, as discussed above. The methyl ester groups, functioning as potential anchor groups for the attachment to semiconductor surfaces, were coupled via standard CuAAC click (see Table 1) reaction on a bipyridine ligand (bpy), which was then chelated to the ruthenium(II) center. While **13a** has a C-connectivity of the anchor group to the $\text{Ru}(\text{bpy})_3$ fragment, **13b** has an N-connectivity. Interestingly, the alternative "chelate then click" pathway starting from an azide or alkyne functionalized ruthenium(II) polypyridine complex could not be persuaded successfully.

Photoactive graphene sheets, which are of high interest for nanoelectronics and photovoltaic systems, were prepared by the "chelate then click" coupling between a ruthenium(II) polypyridine-azide (complex **14**) and an alkyne functionalized graphene.³⁸ The azide group was stabilized by introduction of an intermediary ip system. Corresponding click reaction reported by Zhang et al. is shown in Figure 18 (see Table 1).

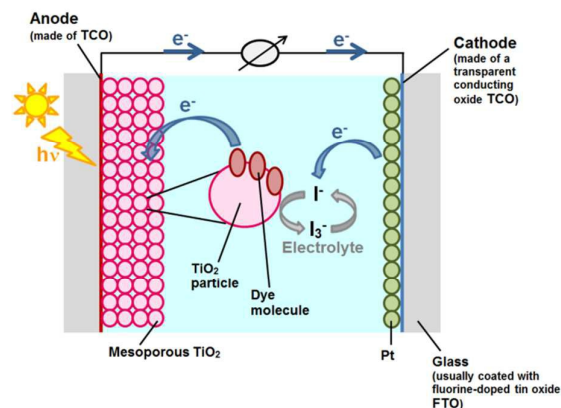


Fig. 16 General function principle of a DSSC.

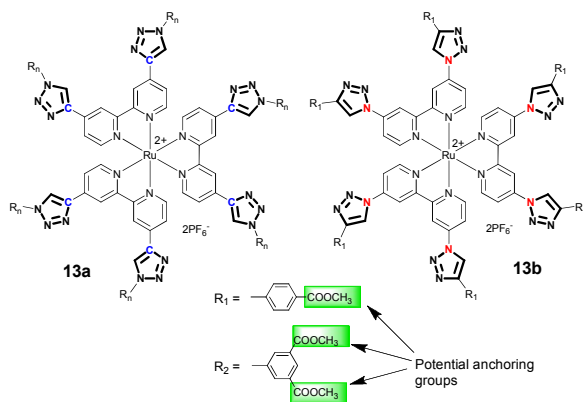


Fig. 17 Complexes **13a** and **13b**, obtained via the „click then chelate“ approach.

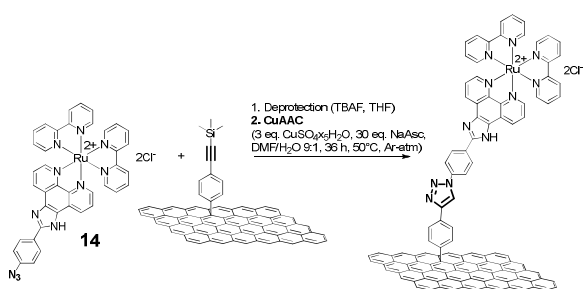


Fig. 18 Generation of a photoactive ruthenium-graphene conjugate via CuAAC click reaction.

Generation of a TiO_2 -attached ruthenium based electron transfer system using the “chelate then click” approach was introduced by Papanikolas (see Figure 19, complex **15**).³⁹ The energy/electron transfer assembly consists of two ruthenium(II) polypyridine cores connected by an oligoproline chain via typical CuAAC (see Table 1). One ruthenium core (Ru-I) is coupled to TiO_2 by phosphonate anchor groups. The other ruthenium core acts as the photosensitizer (Ru-II). After light induced electronic excitation of Ru-II, an energy transfer takes place from Ru-II to Ru-I. After energetic excitation of Ru-I, an electron transfer is induced from Ru-I to the TiO_2 surface.

Schubert et al. introduced alkyl chains to the ruthenium(II) polypyridine complex **16** (Figure 20), using “click to chelate” chemistry (see Table 1), which was tested as a dye for DSSC applications.¹⁴ The maximum overall power conversion efficiency (PCE) was 4.0%, which is comparable to standard dyes, such as the ruthenium based black dye (5.2%). The hydrophobic alkyl chains enhanced the thermal and long term stability by inhibiting water induced photosensitizer desorption.

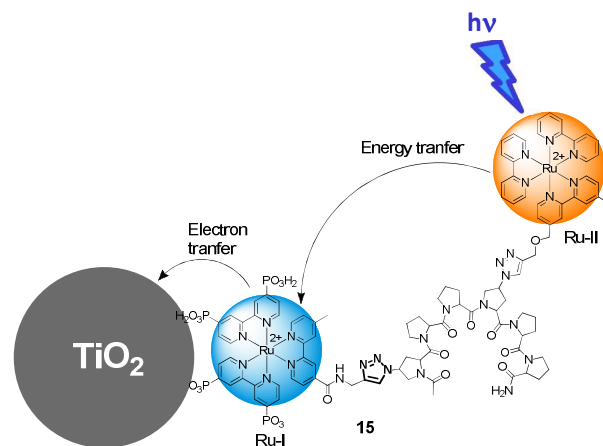


Fig. 19 Mode of action of assembly **15**, which is attached to TiO_2 via phosphonate anchor groups.

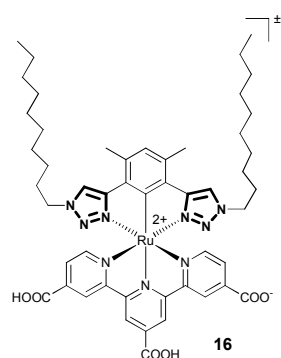


Fig. 20 Complex **16** functioning as the dye in DSSC's applications with PCE = 4.0%.

A PCE of 7.8% could be reached by Bäuerle et al. with the photosensitizer **17**, that was synthesized using the “click to chelate” approach.¹² The CuAAC click reaction was performed using the catalytic system $\text{Cu}(\text{CH}_3\text{CN})_4\text{PF}_6$, Cu^0 and DIPEA (see Table 1). Complex **17** has a broad absorption up to 650 nm with $\lambda_{\text{MLCT}} = 493$ nm ($\epsilon = 7600 \text{ l}\cdot\text{mol}^{-1}\cdot\text{cm}^{-1}$, which is in a typical range for $[\text{Ru}(\text{bpy})_3]^{2+}$ complexes). Emission occurs at 738 nm, which is red shifted compared to $[\text{Ru}(\text{bpy})_3]^{2+}$.

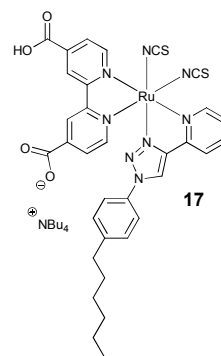


Fig. 21 Complex **17** as a dye for DSSC with PCE = 7.8%.

4.2. Artificial photosynthetic catalysts

While DSSC's transform radiation energy from the sun into electric energy immediately, increasing demand for the storage of solar energy emerges. This issue is being investigated with respect to nature as a role model. At that, plants split water into oxygen and NADPH_2^+ during the photosynthesis. Since hydrogen is an essential component of fuel cells, an imitation of the photosynthesis for the production of hydrogen is highly relevant. Thus, artificial photosynthesis is of great interest in the last decades. Whereas the natural photosynthesis consists of a strongly complicated biomolecular system, the artificial photosynthesis is attempted to be performed with a limited amount of key components. A schematic representation of the water splitting artificial photocatalysis, performed by an intramolecular system, is depicted in Figure 22.⁴⁰ Here, a photosensitizer (PS) is electronically excited by solar light and transfers its electron via a bridging ligand to a reduction catalyst. Thus, protons can be reduced to hydrogen at the reduced catalytic site. At the same time, water is oxidized into oxygen by an oxidation catalyst, that passes the new formed electrons to the oxidized photosensitizer (PS^+) via another bridging ligand regenerating the PS. Afterwards the electron transfer mechanism can be repeated for multiple times. However, the just described mechanism is not trivial, since, among others, two electrons are needed for proton reduction, but four electrons are generated during the water oxidation into oxygen. Therefore, these two half reactions are separated for investigations as a consequence. In the following, we address photocatalytic frameworks that were achieved using CuAAC click reactions.

Natural photosynthesis is based on electron transport systems in protein matrices. Therefore, Leibl et al. investigated the electron transfer between a ruthenium based chromophore and the amino acid tryptophane, connected via the "chelate then click" method (complex **18**).⁴¹ The CuAAC click reaction was performed under standard conditions and with a high yield of 90% (see Table 1). At the presence of an electron acceptor, i.e. methyl viologen, an electron is transferred from the ruthenium(II) moiety towards the electron acceptor A forming A^- and Ru(III). Afterwards an electron transfer from tryptophan to the ruthenium(III) center could be proven, forming Ru(II) and a tryptophan radical after deprotonation of the tryptophan moiety with water as the proton acceptor. In order to accomplish a photocatalytic water oxidation, Stahl et al. performed the coupling between the alkyne-functionalized ruthenium(II) terpyridine complex **9** and an azide terminated diamond electrode within the "chelate then click" approach as well (see Figure 24 and Table 1).²⁹ Complex **9** has been already introduced in chapter 3.3 in Figure 13 for the build-up of alkyne substituted ruthenium complexes. Unfortunately the ruthenium-electrode entity was not stable enough at potentials needed for electrocatalytic water oxidation.

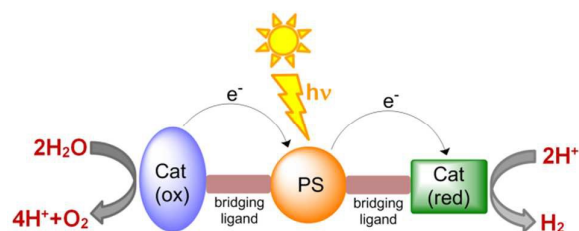


Fig. 22 Working principle of an artificial photocatalytic splitting of water.

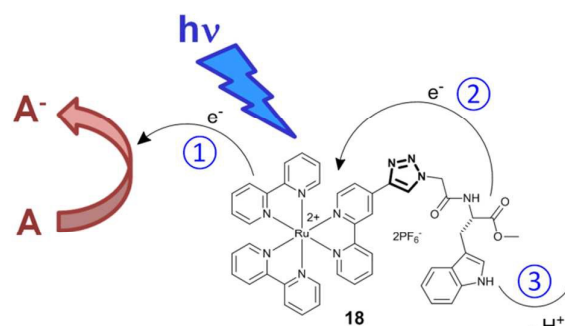


Fig. 23 Photocatalytic electron transfer of a ruthenium(II)-tryptophan conjugate.

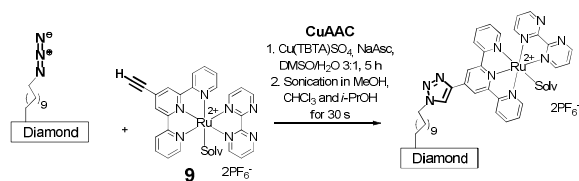


Fig. 24 CuAAC reaction between **9** and an azide functionalized diamond electrode.

The synthesis of a promising photosensitizer for photocatalytic oxidation of water was described by Benniston et al. using the "click then chelate" method.⁴² At that, complex **19** was obtained by attachment of a $\text{Ru}(\text{bpy})_3^{2+}$ moiety to fluoro-borindacene via CuAAC (see Table 1). After addition of the known water oxidation catalyst Ru-CAT, an electron transfer from **19** to an electron acceptor upon photoexcitation and thus water oxidation by Ru-Cat could be shown (see Figure 25). Modulation of a photocatalytic H^+ reducing system using "chelate then click" chemistry was developed by Aukauloo et al (see Figure 26).⁴³ At that, photosensitive ruthenium(II) polypyridine was coupled to the catalytic active nickel cyclam via CuAAC reaction forming **20** (see Table 1). After light irradiation and intramolecular electron transfer from the ruthenium center to the nickel catalyst, a conversion of protons into hydrogen with a TON of 2 respectively was observed. Remarkably, reduction of CO_2 into CO with a TON of 5 succeeded with the same catalytic system as well.

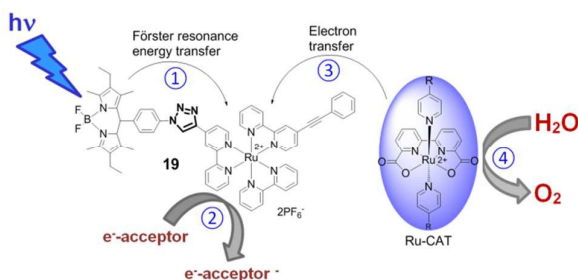


Fig. 25 Theoretical function principle of photocatalytic water oxidation with complex 19 as PS.

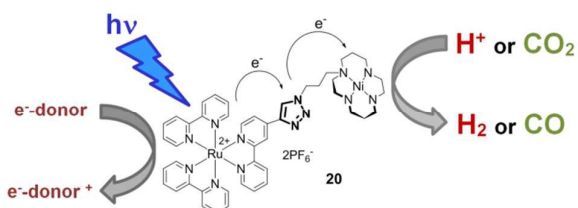


Fig. 26 Photocatalytic reduction of CO₂/H⁺ with a ruthenium(II)-nickel(II)cyclam assembly connected by a triazole linker.

A polymeric intramolecular water photooxidation catalyst with ruthenium(II) chromophores and a ruthenium(II) catalyst was recently developed by T.J. Meyer.⁴⁴ First, azide functionalized polypropylacrylate was formed by reversible addition–fragmentation chain transfer (RAFT) polymerization. Then photoactive alkyne functionalized ruthenium(II) cores were attached to the polymer via “chelate then click” (CuAAC conditions are listed in Table 1). In the final step, a ruthenium(II) polypyridine based water oxidation catalyst Ru(II)-OH₂ was attached as an end group forming compound 21.

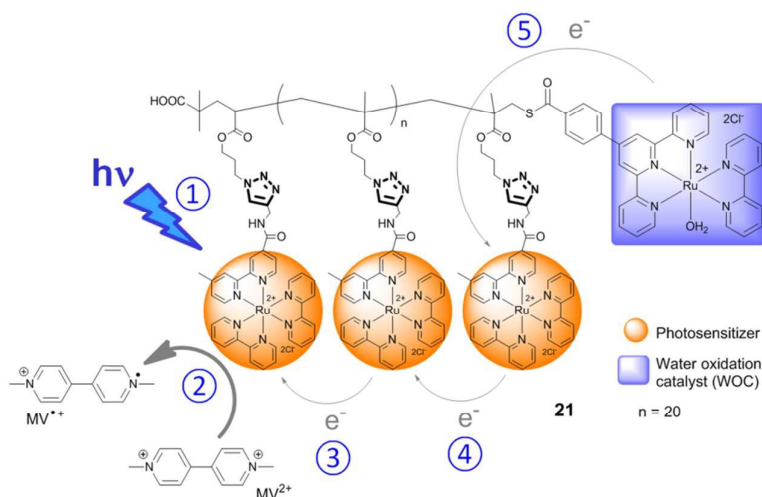


Fig. 27 Photosensitized electron transfer hopping of the polymeric assembly 21

At photoexcitation of the Ru(II) chromophore, excited energy transfer proceeds along the polymer chain forming Ru(II)*. Upon addition of the electron acceptor methylviologen (MV²⁺), an electron transfer from the excited ruthenium(II) photosensitizer Ru(II)* to MV²⁺ takes place, forming Ru(III) and MV^{•+}. Thereafter electron transfer hopping occurs oxidizing the ruthenium(II) chromophores along the chain to Ru(III) until the terminal catalyst is oxidized from Ru(II)-OH₂ to Ru(III)-OH₂. Additionally, the polymeric assembly was attached to nanoparticles such as ZrO₂, TiO₂ and ITO, in order to investigate their applicability for dye sensitized photoelectrosynthesis cells (DSPEC). Thereby electron transfer- and excited state properties are maintained. Nevertheless, the envisaged actual water oxidation is still under investigation.

With the achievements described above, promising steps have been made towards the usage of solar energy. Nevertheless improvements towards higher efficiencies still need to be developed. One possible approach is to enhance the absorbance window of the PS. This may be realized by coupling diversely absorbing PS's into one antenna-like system. Thereby the CuAAC click approach has been already used to synthesize a polymer bearing a photoactive osmium(II) polypyridine and different fluorescent organic moieties. Upon irradiation, an energy transfer from the organic entities to the osmium complex could be observed.⁴⁵ Exploitation of [Ru(bpy)₃]²⁺ based CuAAC click reactions would contribute to the efficiency enhancement of such systems.

5. Photosensitizers generated by CuAAC for therapeutic applications

With the introduction of cisplatin as an anti-cancer chemotherapeutic, transition metal complexes have undergone a vast development in the drug research.⁴⁶ At the generation of a ruthenium based complex, that is capable of undergoing hydrolysis and thus cisplatin-like destruction of DNA, the “click to chelate” concept was used to attach a DNA-interacting ligand to the ruthenium center forming **22**. The ligand was synthesized via CuAAC (see Table 1) and complex **22** generated by chelation.^{47,48}

Nowadays a special interest is given to photoactive transition metal complexes that serve as photosensitizers (PS) in the photodynamic therapy (PDT) against cancer. Upon traditional PDT the initially nontoxic PS generates cell toxic reactive oxygen species (ROS) after activation by light. Thus, spatiotemporal control over tissue destruction is provided representing a great advantage over classical chemotherapy.⁴⁹ At that, ruthenium(II) complexes are great candidates as PS's, due to their capability of electronic activation induced by visible light, leading to reactive species for the formation of singlet oxygen $^1\text{O}_2$ or reduced O_2 equivalents. Complex **23** is one examples where the “click to chelate” concept was used for the generation of possible PS's, as shown in Figure 28.⁵⁰ The conditions of the CuAAC reaction are listed in Table 1.

Still, both chemotherapy and PDT lack specific cancer cell targeting, leading to potentially severe side effects due to additional destruction of healthy cells. Therefore, targeted PDT is very attractive. At that, it is known that some cancer cell types bind predominantly to certain biological groups due to their specific receptor overexpression. Hence, a cancer cell specific biological group can be attached to a potent PS via CuAAC click reaction. Thus the PS-Bio conjugate is explicitly taken up by the corresponding cancer cell type. The mode of action for a targeted PDT is shown in Figure 29.

Upon the coupling of sensitive biological groups on metal complexes the above shown “click to chelate” concept may fail due to the harsh chelating conditions i.e. heating under reflux. Thus it is more advantageous to use the “chelate then click” approach. Therefore, biological groups should be clicked to metal complexes that are functionalized whether with azide- or alkyne groups. Upon condition that non-toxic solvents and catalysts are chosen for the coupling reaction, requirements for a true ‘bioorthogonal’ process would be provided.⁵¹ In general, bioorthogonal reactions are defined as transformations between two abiotic substances that can be performed in physiological systems. At that, they should proceed without assistance of, or interference with the living organism.⁵² For click reactions, a copper free version would have to be used, which however poses some severe limitations of the applicable substitution patterns.

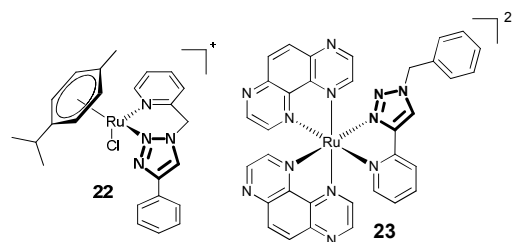


Fig. 28 Complexes **22** for Cisplatin-like destruction of cancer cells and complex **23** for PDT.

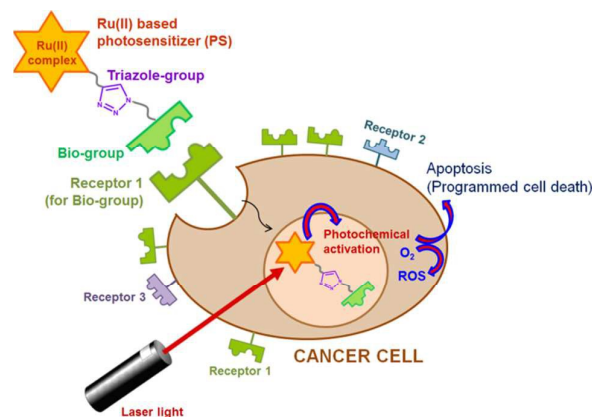


Fig. 29 Mode of action for a targeted PDT.

5.1. Functionalization of biological groups

5.1.1. Generation of Bio-Alkynes

Various reports about the alkylation of biological groups have been shown in literature. Here we restrict to chosen few examples. The introduction of alkynes in amino acids is discussed in a review by S. Pedersen. At that, one feasible method is the direct reduction of the carboxyl group to an aldehyde and subsequent performance of the Colvin-Gilbert-Seyferth reaction (see Figure 30).⁵³

The insertion of the alkyne functionality can be performed at the amino group as well. Here an alkyne coupled NHS (N-hydroxy-succinimide) ester reacts directly with the amino group, as shown in literature in the case of peptides (see Figure 30).⁵⁴

If the amino acid tyrosine is used, a straightforward alkylation method via diazonium coupling can be applied. Within this method Yi et al achieved a one pot alkylation and subsequent CuAAC coupling to a fluorescent agent of the whole protein bovine serum albumin (BSA) and even the tobacco mosaic virus (TMV) that are both known to contain tyrosine.⁵⁵

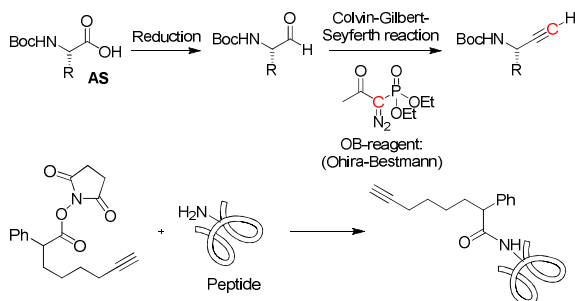


Fig. 30 Introduction of an alkyne functionality to amino acids. At the top: general conversion of a carboxyl group to an alkyne. At the bottom: insertion of an alkyne group to any peptide with an NHS ester.

5.1.2. Formation of Bio-Azides

Multiple examples also exist for the generation of Bio-Azides. Here we report only few selected ones. The preparation of Sugar-Azides out of an acetyl protected gluco-pyranose is typically carried out by a simple reaction with sodium azide.⁵⁶ The azidation of an α -amino-acid is usually performed via diazotransfer reaction at the amino group under basic conditions (see Figure 31). The type of diazotransfer reagent, solvent and base depends on the solubility of the amino acids. The most employed diazotransfer reagents (DTR's) are listed in Figure 31.⁵³ So far, all DTR's are considered as explosive. **DTR1** is most widely employed for the preparation of optically active azide-derived α -amino acids. However, **DTR1** is most explosive. Regarding 'handling, safety and cost', **DTR4** and **DTR5** seem to be more advantageous according to the literature.⁵³ In the case of **DTR2**, **DTR3** and **DTR5**, not enough data has been published for a thorough comparing evaluation. So far, **DTR4** and **DTR5** seem to perform the same azidation reaction as **DTR1** with comparable reaction times and optical purity, but with higher reaction yields and easier handling.

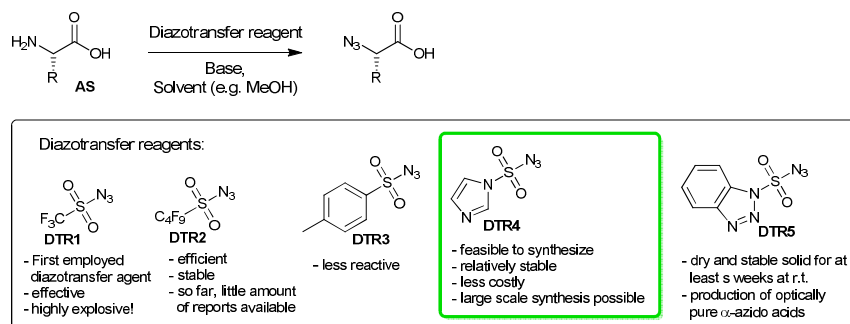


Fig. 31 Azidation of an α -amino acid at the carboxylic group.

5.2. Substitution of functional hormones with azides or alkynes

Hormones are widely employed in clinical chemistry, due to their interaction with specific cell receptors and thus cell signaling pathways.⁵⁷ In this instance we show functionalization methods of two important classes of hormones, i.e. the steroid bile acid and somatostatin. Both can bind to specific receptors of cancer cells and even transport their substituents inside a cell.⁵⁸⁻⁶⁰ Azidation of bile acid is generally performed whether using the carboxylic group (position a) or the hydroxyl functionality (position b), as shown in Figure 32.⁶¹

Alkylation of the bile acid is carried out by amidation or esterification of the carboxylic acid with propargyl amide or propargyl amine respectively within a one-step synthesis (see Figure 32).⁶²

Effective functionalization of somatostatin under retention of its bioactivity has been shown by Weil.^{59, 63} After reductive disulfide bond cleavage of somatostatin, the resulting thiol groups bind to an azide- or alkyne functionalized 'intercalator' **SI-Alkyne** or **SI-N₃** via two successive Michael additions, referred as 'intercalation', as shown in Figure 33. At that, the biologically active group remains intact. Furthermore, stability of the resulting bis-sulfide is even superior compared to the disulfide bond of the native somatostatin.⁵⁹

Dalton Transactions

Perspective

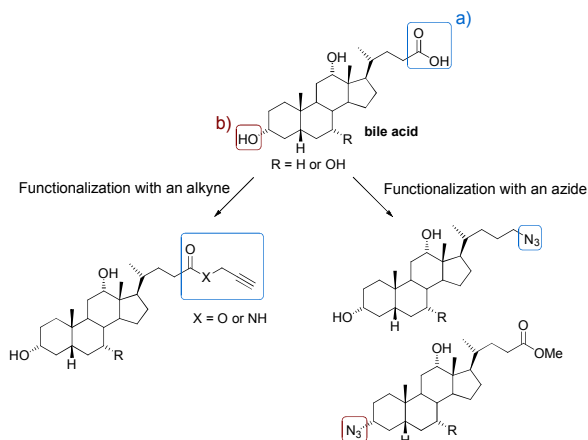


Fig. 32 Introduction of an azide- or alkyne functionality to the estrogen hormone bile acid via position a) or b).

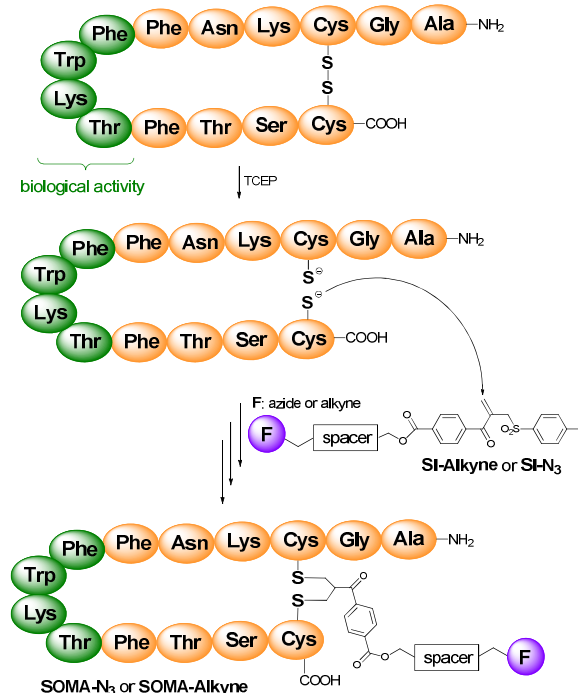


Fig. 33 Intercalation of SI-N₃ or SI-Alkyne generating alkyne- or azide functionalized somatostatin SOMA-N₃/SOMA-Alkyne.

5.3. Attachment of biological groups to Ru(II)-complexes

To the best of our knowledge, so far, only alkyne functionalized [Ru(bpy)₃]²⁺ complexes have been applied for the CuAAC coupling with biological groups. Complex **12** (shown above in Figure 15, chapter 3.3.) was successfully employed for the attachment of peptides by the CuAAC click reaction (depicted in Table 1) forming the conjugate **24**.³³

Coupling of two sugar xylopyranose moieties to a di-alkyne functionalized ruthenium complex was shown by Constable et al.⁶⁴ Here, the ruthenium-alkyne moiety was generated by alkylation with propargyl-bromide of an hydroxo substituted ruthenium(II) polypyridine complex. Thereafter, xylopyranose was clicked via CuAAC (see Table 1) generating complex **25** (see Figure 35).

Recently complex **7c** (see Figure 10) was taken as the reagent for the CuAAC coupling (see Table 1) with a somatostatin-azide forming complex **26** (see Figure 36).⁶⁵ Approaching bioorthogonal click chemistry, the reaction was performed with only water as the solvent. The peptide hormone somatostatin is known to be overly taken up by various cancer cell types due to their overexpression of the receptors SSTR1-5.⁶⁶ Azide-functionalization of somatostatin was shown above in Figure 33. Remarkably, **26** was the first M(II)-Bio conjugate that was both selectively taken up by the cancer cells A549 only due to the somatostatin attachment and could express great phototoxicity.

With respect to biological applications, Cu-ion free reaction conditions are highly interesting, due to the toxic nature of high copper concentrations. The first bioorthogonal strain-promoted copper free azide-alkyne cycloaddition (SPAAC) with a ruthenium(II) polypyridine complex was reported by Lo et al.⁶⁷ Here, an octyne functionality was introduced by amidation (see Figure 37, complex **27**). Additionally, an efficient coupling and photoinduced destruction of cancer cells, that were pretreated with acetyl protected mannose-azide, was performed.

In future ruthenium(II)-Bio conjugates must be optimized towards absorption in the therapeutic window. This can be achieved by either changing the metal center to osmium, or complexation of appropriate ligands, such as phenylpyridine or thiophene-substituted imidazole-phenanthroline.

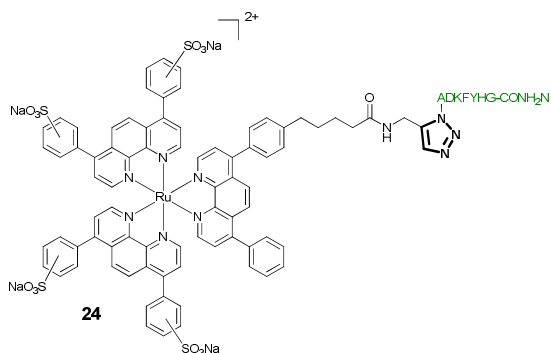


Fig. 34 Complex 24.

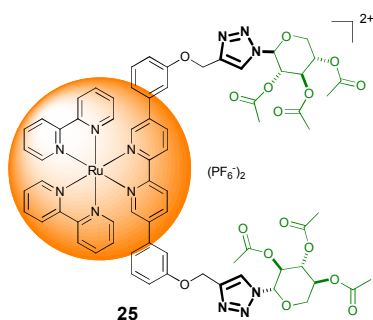


Fig. 35 Complex 25.

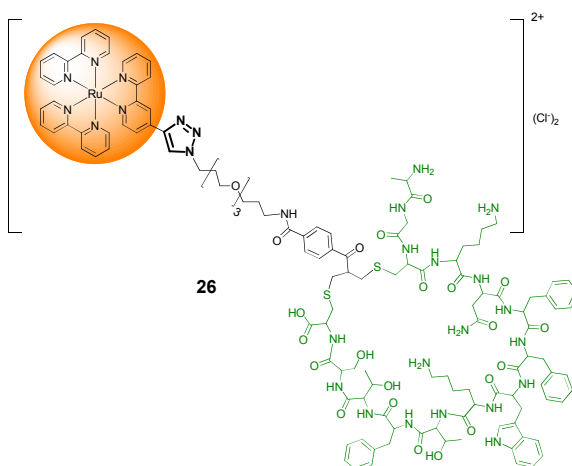


Fig. 36 Ruthenium-somatostatin conjugate 26.

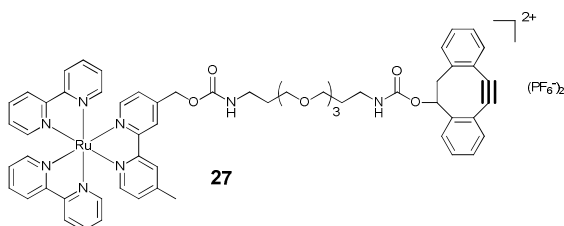


Fig. 37 Complex 27.

Conclusions

We have discussed three methods, used in literature for performing CuAAC click reactions with ruthenium(II) complexes, which are “click to chelate”, “click then chelate” and “chelate then click”.

The first two are mostly employed for the generation of photosensitizers (PS's) for DSSC's or photocatalysts. This way the expensive ruthenium compound is spared by introduction in the last step via chelation. The “chelate then click” approach is predominantly applied for the formation of PS's for photodynamic applications, in order to avoid destruction of the sensitive biologically active compounds.

Generally if working with the “click to chelate” method, possible luminescence quenching has to be taken into account. Upon chelation with azide bearing ligands, destruction of the azide group may occur. Therefore spacers such as methylene or imidazole-phenanthroline (ip) can be successfully applied. At the chelation of alkyne bearing ligands, severe side products containing Ru-CO occur, if standard chelation conditions are used. The side reactions can be avoided by whether using Ag^+ ions and protection of the alkyne group, or introduction of the alkyne group to a ruthenium complex lacking labile ligands.

With the employment of click reactions, a DSSC with PCE = 7.8 %, photocatalysts for the formation of H_2 or conversion of CO_2 and a cancer cell selective PS for PDT treatment could be generated.

Table 1. Summary of discussed CuAAC click reaction.

Figure/complex	Conditions	Ref.
Fig. 4/ 1 (ligand)	10 mol% CuSO ₄ ·5H ₂ O, 100 mol% sodium ascorbate, EtOH/H ₂ O 2:1, 24 h, r.t., yield: 86%	13
Fig. 6/ 3a-c (ligand)	5 mol% CuSO ₄ ·5H ₂ O, 10 mol% sodium ascorbate, CH ₂ Cl ₂ /H ₂ O (1:1), 20 h, r.t. (3c : 2 d, 130°C), yield: 96-98%	20
Fig. 7/ 4a-c	CuSO ₄ ·5H ₂ O, sodium ascorbate, THF/H ₂ O (1:1), 12 h, r.t., yield: 47-80%	24
Fig. 8/ 5a-b (ligand)	0.36 eq CuSO ₄ ·5H ₂ O, 0.89 eq. sodium ascorbate, CH ₂ Cl ₂ /H ₂ O 1:1, 12 h, yield: 30-53%.	25
Fig. 9/ 6	0.15 eq. CuSO ₄ ·5H ₂ O, 0.45 eq. sodium ascorbate, CH ₂ Cl ₂ /H ₂ O 1:1, r.t. 4 d, yield: 55%	26
Fig. 12/ 8a-c	15 mol% CuSO ₄ ·5H ₂ O, 45 mol% sodium ascorbate, CH ₂ Cl ₂ /H ₂ O 1:1, 20h, r.t, yield: 58-81%	28
Fig. 14/ 11a-b	1 eq. CuBr, 1 eq. PMDETA, DMF, Ar, r.t., 44 h, 36-50%	32
Fig. 17/ 13a-b (ligand)	0.2 eq. CuSO ₄ ·5H ₂ O/ 0.6 eq. sodium ascorbate, (iPr) ₃ EtN, H ₂ O, H ₂ O/ <i>t</i> -BuOH/MeOH 1:2:1, N ₂ , r.t., 18 h, yield: 47%	37
Fig. 18/ (CuAAC with 14)	3 eq. CuSO ₄ ·5H ₂ O, 30 eq. sodium ascorbate, DMF/H ₂ O 9:1, Ar, 50°C, 36 h, yield: highly efficient	38
Fig. 19/ 15	2 eq. CuSO ₄ ·5H ₂ O, 8 eq. sodium ascorbate, EtOH/H ₂ O 1:1, 12 h, r.t., yield: n.s.	39
Fig. 20/ 16 (ligand)	4 mol% CuSO ₄ ·5H ₂ O, 32 mol% sodium ascorbate, EtOH/H ₂ O 2:1, 2 h, 50°C, yield: 85%	14
Fig. 21/ 17 (ligand)	Cu(CH ₃ CN) ₄ PF ₆ ⁻ , Cu ⁰ , DIPEA, CH ₂ Cl ₂ /MeOH 4:1, 3 d, r. t., yield: 89%	12
Fig. 23/ 18	15 mol% CuSO ₄ ·5H ₂ O, 45 mol% sodium ascorbate, CH ₂ Cl ₂ /H ₂ O 1:1, 20 h and r. t, yield: 90%	41
Fig. 24/ (CuAAC with 9)	eq. Cu(TBTA)SO ₄ , eq. sodium ascorbate, DMSO/H ₂ O 3:1, sonification, 5 h, yield: n.s.	29
Fig. 25/ 19 (ligand)	1 eq. CuSO ₄ ·5H ₂ O, 10 eq. sodium ascorbate, MeCN/H ₂ O 1:1, 18 h and 40°C, yield: 63%	42
Fig. 26/ 20	CH ₂ Cl ₂ /H ₂ O 1:1, 0.15 eq. CuSO ₄ ·5H ₂ O, 0.45 eq. sodium ascorbate, Ar, r.t. overnight, yield: 81%	43
Fig. 27/ 21	CuBr, DMF, PMDETA, 100°C, stirring overnight, yield: 81%	44
Fig. 28/ 22 (ligand)	87 mol% CuSO ₄ ·5H ₂ O, 315 mol% granular copper, MeOH/H ₂ O 2:1, 1.5 h, yield: 93%	48
Fig. 28/ 23 (ligand)	0.4 eq. CuSO ₄ , 1.3 eq. sodium ascorbate, <i>t</i> -BuOH/water 1:1, 24 h, r. t., inert atm, yield 78%	50
Fig. 34/ 24	5.2 eq. CuSO ₄ ·5H ₂ O, 10 eq. sodium ascorbate, 10 eq. TBTA, 5.2 eq. DIPEA, DMSO, 25°C, stirring overnight, yield: complete conversion	33
Fig. 35/ 25	20 eq. CuSO ₄ ·5H ₂ O, 10 eq. sodium ascorbate, DMF, N ₂ , r.t. 3 d, yield: 93%	64
Fig. 36/ 26	2 eq. CuSO ₄ ·5H ₂ O, 4 eq. sodium ascorbate, H ₂ O, 24 h, r.t., yield: 61%, complete conversion	65

Acknowledgements

We thank the Landesgraduiertenförderungsgesetz (LGFG) University Ulm for financial support.

Notes and references

‡ Footnotes relating to the main text should appear here. These might include comments relevant to but not central to the matter under discussion, limited experimental and spectral data, and crystallographic data.

§
§§
etc.

1. A. Juris, V. Balzani, F. Barigelletti, S. Campagna, P. Belser and A. von Zelewsky, *Coordination Chemistry Reviews*, 1988, **84**, 85-277.
2. H. C. Kolb, M. G. Finn and K. B. Sharpless, *Angewandte Chemie International Edition*, 2001, **40**, 2004-2021.
3. F. Himo, T. Lovell, R. Hilgraf, V. V. Rostovtsev, L. Noodleman, K. B. Sharpless and V. V. Fokin, *Journal of the American Chemical Society*, 2005, **127**, 210-216.
4. V. Aucagne, K. D. Hänni, D. A. Leigh, P. J. Lusby and D. B. Walker, *Journal of the American Chemical Society*, 2006, **128**, 2186-2187.
5. V. Balzani and S. Campagna, *Photochemistry and Photophysics of Coordination Compounds I*, Springer, Berlin, 2007.
6. P. S. Wagenknecht and P. C. Ford, *Coordination Chemistry Reviews*, 2011, **255**, 591-616.
7. V. Balzani, P. Ceroni and A. Juris, *Photochemistry and Photophysics: Concepts, Research, Applications*, John Wiley & Sons, Weinheim, 2014.
8. K. Suzuki, A. Kobayashi, S. Kaneko, K. Takehira, T. Yoshihara, H. Ishida, Y. Shiina, S. Oishi and S. Tobita, *Physical Chemistry Chemical Physics*, 2009, **11**, 9850-9860.
9. C. Tanielian, C. Wolff and M. Esch, *The Journal of Physical Chemistry*, 1996, **100**, 6555-6560.
10. C. Zhang, X. Shen, R. Sakai, M. Gottschaldt, U. S. Schubert, S. Hirohara, M. Tanihara, S. Yano, M. Obata, N. Xiao, T. Satoh and T. Kakuchi, *Journal of Polymer Science Part A: Polymer Chemistry*, 2011, **49**, 746-753.
11. B. B. Kasten, X. Ma, H. Liu, T. R. Hayes, C. L. Barnes, S. Qi, K. Cheng, S. C. Bottorff, W. S. Slocumb, J. Wang, Z. Cheng and P. D. Benny, *Bioconjugate Chemistry*, 2014, **25**, 579-592.
12. I. Stengel, A. Mishra, N. Pootrakulchote, S.-J. Moon, S. M. Zakeeruddin, M. Gratzel and P. Bauerle, *Journal of Materials Chemistry*, 2011, **21**, 3726-3734.
13. B. Schulze, C. Friebe, S. Hoepfener, G. M. Pavlov, A. Winter, M. D. Hager and U. S. Schubert, *Macromol. Rapid Commun.*, 2012, **33**, 597-602.
14. B. Schulze, D. G. Brown, K. C. D. Robson, C. Friebe, M. Jäger, E. Birkner, C. P. Berlinguette and U. S. Schubert *Chemistry – A European Journal*, 2013, **19**, 1521-3765.
15. B. Schulze, C. Friebe, M. D. Hager, A. Winter, R. Hoogenboom, H. Gorus and U. S. Schubert, *Dalton Transactions*, 2009, 787-794.

16. U. Monkowius, S. Ritter, B. König, M. Zabel and H. Yersin, *European Journal of Inorganic Chemistry*, 2007, **2007**, 4597-4606.
17. Y. Chen, N. Xiao, T. Satoh and T. Kakuchi, *Polymer Chemistry*, 2014, **5**, 4993-5001.
18. J. P. Byrne, J. A. Kitchen, O. Kotova, V. Leigh, A. P. Bell, J. J. Boland, M. Albrecht and T. Gunnlaugsson, *Dalton Transactions*, 2014, **43**, 196-209.
19. S. Hohloch, D. Schweinfurth, M. G. Sommer, F. Weisser, N. Deibel, F. Ehret and B. Sarkar, *Dalton Transactions*, 2014, **43**, 4437-4450.
20. A. Baron, C. Herrero, A. Quaranta, M.-F. Charlot, W. Leibl, B. Vauzeilles and A. Aukauloo, *Chemical Communications*, 2011, **47**, 11011-11013.
21. S. Rau, B. Schäfer, A. Grüßing, S. Schebesta, K. Lamm, J. Vieth, H. Görls, D. Walther, M. Rudolph, U. W. Grummt and E. Birkner, *Inorganica Chimica Acta*, 2004, **357**, 4496-4503.
22. B. Schulze and U. S. Schubert, *Chemical Society Reviews*, 2014, **43**, 2522-2571.
23. B. Happ, D. Escudero, M. D. Hager, C. Friebe, A. Winter, H. Görls, E. Altuntaş, L. González and U. S. Schubert, *The Journal of Organic Chemistry*, 2010, **75**, 4025-4038.
24. B. S. Uppal, A. Zahid and P. I. P. Elliott, *European Journal of Inorganic Chemistry*, 2013, **2013**, 2571-2579.
25. M. Braumüller, D. Sorsche, M. Wunderlin and S. Rau, *European Journal of Organic Chemistry*, 2015, **2015**, 5987-5994.
26. A. Kroll, K. Monczak, D. Sorsche and S. Rau, *European Journal of Inorganic Chemistry*, 2014, **2014**, 3462-3466.
27. N. Zabarska, D. Sorsche, F. W. Heinemann, S. Glump and S. Rau, *European Journal of Inorganic Chemistry*, 2015, **2015**, 4869-4877.
28. A. Baron, C. Herrero, A. Quaranta, M.-F. Charlot, W. Leibl, B. Vauzeilles and A. Aukauloo, *Inorganic Chemistry*, 2012, **51**, 5985-5987.
29. J. B. Gerken, M. L. Rigsby, R. E. Ruther, R. J. Pérez-Rodríguez, I. A. Guzei, R. J. Hamers and S. S. Stahl, *Inorganic Chemistry*, 2013, **52**, 2796-2798.
30. S. J. Slade and G. F. Pegg, *Annals of Applied Biology*, 1993, **122**, 233-251.
31. H. T. Ratte, *Environmental Toxicology and Chemistry*, 1999, **18**, 89-108.
32. Y. Sun, Z. Chen, E. Puodziukynaite, D. M. Jenkins, J. R. Reynolds and K. S. Schanze, *Macromolecules*, 2012, **45**, 2632-2642.
33. M. C. Uzagare, Clau, M. Gerrits and W. Bannwarth, *Organic & Biomolecular Chemistry*, 2012, **10**, 2223-2226.
34. A. Juris, V. Balzani, F. Barigletti, S. Campagna, P. Belser and A. von Zelewsky, *Coordination Chemistry Reviews*, 1988, **84**, 85-277.
35. A. Hagfeldt, G. Boschloo, L. Sun, L. Kloo and H. Pettersson, *Chemical Reviews*, 2010, **110**, 6595-6663.
36. E. A. Gibson, A. L. Smeigh, L. Le Pleux, L. Hammarström, F. Odobel, G. Boschloo and A. Hagfeldt, *The Journal of Physical Chemistry C*, 2011, **115**, 9772-9779.
37. K. P. Chitre, E. Guillén, A. S. Yoon and E. Galoppini, *European Journal of Inorganic Chemistry*, 2012, **2012**, 5461-5464.
38. H.-X. Wang, K.-G. Zhou, Y.-L. Xie, J. Zeng, N.-N. Chai, J. Li and H.-L. Zhang, *Chemical Communications*, 2011, **47**, 5747-5749.
39. D. Ma, S. E. Bettis, K. Hanson, M. Minakova, L. Alibabaei, W. Fondrie, D. M. Ryan, G. A. Papoian, T. J. Meyer, M. L. Waters and J. M. Papanikolas, *Journal of the American Chemical Society*, 2013, **135**, 5250-5253.
40. S. Kauffhold, L. Petermann, R. Staehle and S. Rau, *Coordination Chemistry Reviews* 2015, **304-305**, 73-87.
41. S. Sheth, A. Baron, C. Herrero, B. Vauzeilles, A. Aukauloo and W. Leibl, *Photochemical & Photobiological Sciences*, 2013, **12**, 1074-1078.
42. P. Farràs and A. C. Benniston, *Tetrahedron Letters*, 2014, **55**, 7011-7014.
43. C. Herrero, A. Quaranta, S. El Ghachtouli, B. Vauzeilles, W. Leibl and A. Aukauloo, *Physical Chemistry Chemical Physics*, 2014, **16**, 12067-12072.
44. Z. Fang, A. Ito, H. Luo, D. L. Ashford, J. J. Concepcion, L. Alibabaei and T. J. Meyer, *Dalton Transactions*, 2015, **44**, 8640-8648.
45. A. M. Breul, I. Rabelo de Moraes, R. Menzel, M. Pfeffer, A. Winter, M. D. Hager, S. Rau, B. Dietzek, R. Beckert and U. S. Schubert, *Polymer Chemistry*, 2014, **5**, 2715-2724.
46. N. P. E. Barry and P. J. Sadler, *Chemical Communications*, 2013, **49**, 5106-5131.
47. I. Bratsos, D. Urankar, E. Zangrando, P. Genova-Kalou, J. Kosmrlj, E. Alessio and I. Turel, *Dalton Transactions*, 2011, **40**, 5188-5199.
48. D. Urankar, B. Pinter, A. Pevec, F. De Proft, I. Turel and J. Košmrlj, *Inorganic Chemistry*, 2010, **49**, 4820-4829.
49. J. D. Knoll and C. Turro, *Coordination Chemistry Reviews*, 2015, **282-283**, 110-126.
50. A. Mattiuzzi, I. Jabin, C. Moucheron and A. Kirsch-De Mesmaeker, *Dalton Transactions*, 2011, **40**, 7395-7402.
51. M. Yang, J. Li and P. R. Chen, *Chemical Society Reviews*, 2014, **43**, 6511-6526.
52. M. Boyce and C. R. Bertozzi, *Nat Meth*, 2011, **8**, 638-642.
53. H. Johansson and D. S. Pedersen, *European Journal of Organic Chemistry*, 2012, **2012**, 4267-4281.
54. A. O.-Y. Chan, C.-M. Ho, H.-C. Chong, Y.-C. Leung, J.-S. Huang, M.-K. Wong and C.-M. Che, *Journal of the American Chemical Society*, 2012, **134**, 2589-2598.
55. J. Zhang, D. Ma, D. Du, Z. Xi and L. Yi, *Organic & Biomolecular Chemistry*, 2014, **12**, 9528-9531.
56. M. Pocchi, S. Alfei, F. Lucchesini, V. Bertini and B. Idini, *Tetrahedron*, 2009, **65**, 5684-5692.
57. B. S. Katzenellenbogen, *Biology of Reproduction*, 1996, **54**, 287-293.
58. J. Hu, J. R. Lu and Y. Ju, *Chemistry – An Asian Journal*, 2011, **6**, 2636-2647.
59. T. Wang, D. Y. W. Ng, Y. Wu, J. Thomas, T. TamTran and T. Weil, *Chemical Communications*, 2014, **50**, 1116-1118.
60. X. Wang, X. Fu, C. Van Ness, Z. Meng, X. Ma and W. Huang, *Current pathobiology reports*, 2013, **1**, 29-35.
61. V. S. Pore, N. G. Aher, M. Kumar and P. K. Shukla, *Tetrahedron*, 2006, **62**, 11178-11186.
62. N. S. Vatmurge, B. G. Hazra, V. S. Pore, F. Shirazi, M. V. Deshpande, S. Kadreppa, S. Chattopadhyay and R. G.

ARTICLE

Journal Name

- Gonnade, *Organic & Biomolecular Chemistry*, 2008, **6**, 3823-3830.
63. T. Wang, Y. Wu, S. L. Kuan, O. Dumele, M. Lamla, D. Y. W. Ng, M. Arzt, J. Thomas, J. O. Mueller, C. Barner-Kowollik and T. Weil, *Chemistry – A European Journal*, 2015, **21**, 228-238.
64. E. C. Constable, C. E. Housecroft, M. Neuburger and P. Rosel, *Chemical Communications*, 2010, **46**, 1628-1630.
65. T. Wang, N. Zabarska, Y. Wu, M. Lamla, S. Fischer, K. Monczak, D. Y. W. Ng, S. Rau and T. Weil, *Chemical Communications*, 2015, **51**, 12552-12555.
66. S. LC and C. DH, *Current Drug Delivery*, 2011, **8**, 2-10.
67. T. S.-M. Tang, A. M.-H. Yip, K. Y. Zhang, H.-W. Liu, P. L. Wu, K. F. Li, K. W. Cheah and K. K.-W. Lo, *Chemistry – A European Journal*, 2015, **21**, 10729-10740.